Journal of
Materials Chemistry B

Accepted Manuscript

This article can be cited before page numbers have been issued, to do this please use: C. A. Choi, Z. A. I. Mazrad, J. H. Ryu, I. In, K. D. Lee and S. Y. Park, *J. Mater. Chem. B*, 2018, DOI: 10.1039/C8TB01364K.

ROYAL SOCIETY OF CHEMISTRY

rsc.li/materials-b

Journal of

Materials Chemistry B

Article Online
DOI: 10.1039/C8TB01364K
JOURNAL OF CHEMISTRY

ARTICLE

Membrane and nucleus targeting for highly sensitive cancer cell detection using pyrophosphate and alkaline phosphatase activity-mediated fluorescence switching of functionalized carbon dot

Received 00th January 20xx,
Accepted 00th January 20xx

DOI: 10.1039/x0xx00000x

www.rsc.org/

Cheong A Choi[a], Zihnil Adha Islamy Mazrad[b], Ji Hyun Ryu[c], Insik In[b,d] , Kang Dae Lee[e*], and Sung Young Park[a,b*]

A specific membrane and nucleus targeted fluorescence OFF-ON-OFF system using the dodecane/sulfobetaine group of functionalized carbon dot (CD) with a copper ion (Cu^{2+}-CD) based on the presence of pyrophosphate (PPi) molecules and alkaline phosphatase (ALP) activity, for cancer cell detection was designed. The biosensor could be effectively transported from the cytosol to the nucleus in MDAMB cells, but not in MDCK cells due to the response to change in pH by CD functionalized with zwitterionic groups. The biosensor also showed a membrane-selective regulated route for fusion of long alkyl chain grafted-CD on cell membranes. As a potential sensor, the fluorescence of the prepared Cu^{2+}-CD was significantly quenched due to aggregation. In human cancer MDAMB cells, a nearly complete restoration of fluorescence intensity of the Cu^{2+}-CD was observed because of the high levels of intracellular PPi, which preferentially bind to Cu^{2+}. After 10 min, in the MDAMB cells, re-quenching of the CD fluorescence occurred because of the high level of intracellular ALP, which can hydrolyze PPi and release the Cu^{2+} to re-aggregate the CD. In contrast to MDAMB cells, MDCK cells did not show an obvious response to the specific intracellular biomolecules, thus, enabling the biosensor to be used to distinguish between cancer and normal cells. In conclusion, this biosensor has the potential to be a simple and sensitive cancer diagnostic tool that can differentiate normal cells from cancer cells on coated surfaces and in aqueous states.

Introduction

Highly sensitive and selective assays with the potential for clinical diagnoses are required, especially for tumor detection. However, most reported technological innovations generally require a long detection time and complex preparation and are subject to numerous limitations, including low sensitivity.[1,2] For practical applications in tumor detection, rapid cell penetration is essential to avoid sample inactivation or photobleaching; therefore, a system with rapid selective membrane binding is required.[3-6] Cell membranes mainly consist of phospholipids, which make it easy for hydrophobic masses to be taken up into the hydrophobic region of cell membranes and tightly intercalate into the lipid bilayer.[7] However, most nanomaterials for cell treatment are localized in the cell cytoplasm, which is not effective if the system carries a therapeutic agent.[8-11] As an alternative, zwitterionic substances, with both positively and negatively charged functional groups, can support cytoplasmic uptake and subsequent nuclear internalization, triggered by a change in pH.[12-14] Consequently, there is an urgent need to develop simple, cost effective, sensitive, and rapid tumor markers with selective membrane binding capacity and appropriate cellular uptake mechanism that will not be trapped in the cell cytoplasm.

In case of specific detection, pyrophosphate (PPi), a hydrolysis product of adenosine triphosphate, has a key role in energy transduction and several major metabolic processes and can be used in cancer diagnosis.[15-16] Alkaline phosphatase (ALP), one of the most commonly used hydrolase enzymes found in various mammalian organs (e.g., bone, liver, placenta, and intestines), can hydrolyze the PPi to Pi form.[17-19] Additionally, the concentrations of PPi and ALP are different in the normal and diseased states, making them potential targets to differentiate normal cells from cancer cells.[20-21] Till date, research focused on developing cancer detection methods using PPi and ALP has involved colorimetric, fluorometric,

[a] Department of Chemical & Biological Engineering, Korea National University of Transportation, Chungju 380-702, Republic of Korea.
[b] Department of IT Convergence, Korea National University of Transportation Chungju 380-702, Republic of Korea.
[c] Department of Carbon Fusion Engineering, Wonkwang University, Iksan, Jeonbuk 54538, South Korea
[d] Department of Polymer Science and Engineering, Korea National University of Transportation, Chungju 380-702, Republic of Korea.
[e] Department of Otolaryngology–Head and Neck Surgery, Kosin University College of Medicine, Busan 49267, Republic of Korea.
Corresponding Authors
*E-mail: parkchem@ut.ac.kr (Sung Young Park), Fax number: 043-841-5220
kdlee59@gmail.com (Kang Dae Lee)
Electronic Supplementary Information (ESI) available: [details of any supplementary information available should be included here]. See DOI: 10.1039/x0xx00000x

surface-enhanced Raman scattering, and electrochemical methods.[22-24] Among them, studies have reported the use of organic dyes, fluorescent polymers, and metal nanoclusters or nanoparticles as on/off biomarkers; however, there are limitations in the practical application of these methods because of their stability, synthesis method, and high cost. Moreover, there are no reports of tumor selective membrane- and nucleus-targeted diagnostic assays using a fluorometric on/off system in response to PPi and ALP activity.

Carbon dot (CD) have been used extensively for fluorometric assays because of their excellent photoluminescence (PL), high chemical stability, low toxicity, anti photobleaching properties, environmental friendliness, low cost, and good biocompatibility.[25-27] Moreover, they can also be modified with signal molecules or fluorescence resonance energy transfer (FRET) pairs to obtain a fluorescent on/off system.[28-30] Commonly, when CD interact with metals, including Cu^{2+}, Zn^{2+}, and Fe^{3+}, the PL of the CD is significantly quenched.[31-33] Additionally, there is a unique chelation interaction between PPi and metal ions that can be hydrolyzed by ALP, which affects the fluorescence of the CD.[34] Consequently, the design of CD integrated with metal ion was suggested as a promising system to detect cancer cells in response to intracellular PPi and ALP activity.

In the present study, we designed a membrane/nucleus specific targeted fluorescent OFF-ON-OFF sensing system in aqueous and coated surfaces for tumor-selective detection. The system is based on the response of carbonized hydrophobic dodecane chain, adhesive catechol, and zwitterionic sulfobetaine quaternized polymers (CD) to levels of PPi and ALP activity in cancer cells. The CD exhibit great potential for tumor-triggered detection assays in solution and on coated surfaces. The designed assay can effectively and selectively distinguish between tumor and normal cells with high sensitivity and is a rapid colorimetric assay for other clinical diagnostic tests.

EXPERIMENTAL SECTION

Materials and characterization

Polyethylene glycol (PEG; Mw 3,350), 2-dimethylaminoethyl methacrylate (DMA), t-butyl peroxybenzoate, bromododecane (C_{12}), 2-chloro-3', 4'-dihydroxy acetonephenone (CCDP, a catechol derivative), bromo dodecane, 1,3-propanesultone, anhydrous tetrahydrofuran (THF), toluene, hexane, ethanol (EtOH), diethyl ether, concentrated H_2SO_4, double-deionized water (DDW), copper solution (10 mM), alkaline phosphatase (ALP), pyrophosphates (PPi) (10 mM), Trizma base (TBS), [3-(4,5-dimethylthiazol-2-yl)-2,5-diphenyltetrazolium bromide] (MTT), and sodium metavanadate (Na_3VO_4, as an ALP inhibitor) were purchased from Sigma Aldrich, Korea. Penicillin-streptomycin, fetal bovine serum (FBS), 0.25% (w/v) trypsin, 0.05% (w/v) EDTA solution, and Roswell Park Memorial Institute (RPMI)-1640 medium were purchased from Gibco BRL (Carlsbad, CA, USA). Fluorescein isothiocyanate (FITC) Annexin V and propidium iodide (PI) were purchased from Invitrogen (USA). MDAMB and MDCK cells were obtained from the Korean Cell Line Bank (Seoul, Korea). Solid substrates, namely, silicon wafer (Si), poly-(ethylene terephthalate) (PET), polyvinylchloride (PVC), polystyrene (PS), and polypropylene (PP) were prepared, according to the protocols reported in a previous study.

^1H nuclear magnetic resonance (NMR) spectra were recorded on a 400 MHz Bruker Advance spectrometer (Bruker Corp., Billerica, MA, USA) using deuterium oxide (D_2O) and deuterium dimethyl sulfoxide (DMSO-d_6) as solvents. The ultraviolet-visual (UV-vis) spectra were recorded using an Optizen 2020UV spectrophotometer (Mecasys Co.). X-ray diffraction (XRD) was performed using a D-8 ADVANCE X-ray diffractometer (Bruker Corp). Particle size was measured by dynamic light scattering (DLS) (Zetasizer Nano, Malvern, Kassel, Germany). PL spectra were obtained using a Perkin Elmer L550B luminescence spectrometer. A multimode microplate reader, Filter MaxF3 (Molecular Devices, LLC.), was used for the MTT assay. Flow cytometry data (fluorescence-activated cell sorting, FACS) was recorded using an Attune NxT Acoustic Focusing Cytometer (Thermo Scientific, USA). Fluorescence images were observed using L550B luminescence spectrometer (Perkin Elmer, Waltham, MA, USA) and an LSM510 Confocal Laser-scanning Microscope (CLSM; Carl Zeiss, Germany) equipped with a 364 nm UV laser and a 543 nm He/Ne laser. The water contact angle of surfaces coated with material was measured on a DO3210 instrument (KRUSS DSA 100 Optima system, KRUSS, Hamburg, Germany). The dodecane/catechol quaternized poly (ethylene glycol)-g-poly (2-dimethylaminoethyl methacrylate) (C/C_{12}-PEG-g-PDMA) was obtained using a method similar to that reported in our previous study.[28]

Synthesis of dodecane and zwitterion functionalized surface-coatable fluorescent carbon dots (CD)

The sulfobetaine grafted C/C_{12}-PEG-g-PDMA (C/C_{12}-SP) was obtained, using a similar method reported previously.[28] Briefly, C/C_{12}-PEG-g-PDMA (4.465×10^{-5}, 5 g) was dissolved in ethanol (80 mL), and 1,3-propanesultone (8.92×10^{-5},0.78 mL) was diluted with THF (30 mL), respectively. After that, the solution was stirred at 30–40°C for 12 h. At the end of the reaction, the solution was evaporated using a rotary evaporator and precipitated with diethyl ether. The sample was collected after drying in a vacuum oven. Finally, CD was obtained by an acid-assisted carbonization method at room temperature for 1 min with continuous magnetic stirring. Dialysis was performed (molecular weight cut off = 1 kDa) against DDW, and the CD were then freeze-dried for 2 days.

Synthesis of copper-complexed fluorescent carbon dots (Cu^{2+}-CD)

To optimize the amount Cu^{2+} needed for the quenching effect, varying volumes of copper solution (0, 5, 10, 20, 40, 60

View Article Online
DOI: 10.1039/C8TB01364K

µL) (10 mM) were mixed with the CD solution in DDW (5 mg/mL), and then the PL was determined after 24 h of incubation at room temperature. For characterization and the PPi detection assay, 60 µL of copper solution (10 mM) was used. The product was confirmed using UV-Vis spectroscopy, PL detection, and XRD.

Fluorescence recovery *via* a PPi detection assay

The concentration of PPi required to recover the fluorescence intensity was optimized.in particular, different volumes of PPi solutions (0, 5, 10, 20, 30, 50, 100 µL) (10 mM) were mixed with the Cu^{2+}-CD solution (1 mg/mL), and the mixture was shaken for 5 min at room temperature. The successful interaction between Cu^{2+}-CD and PPi was confirmed by XRD, and the recovered fluorescence intensity was recorded as the PL at an excitation wavelength of 380 nm.

Fluorescence OFF by ALP activity

Briefly, 1 mL of DDW containing Cu^{2+}-CD+PPi (1 mg/mL) was added to solutions containing different concentrations of ALP solution (60, 125, 250, 500, and 1000 U/L) and shaken at room temperature for 10 min. Thereafter, the emission spectra of the solutions were recorded at an excitation wavelength of 380 nm.

Surface coating with various substrates

Several kinds of solid substrates (PP, PET, PVC, PS, and Si) were prepared using dip coating methods. Surfaces were coated with CD, Cu^{2+}-CD, Cu^{2+}-CD+PPi, and Cu^{2+}-CD+PPi+ALP by immersing the substrate surface in a TBS solution (pH 8.5) containing 10 mg/mL of coating materials at room temperature for 24 h. Thereafter, the coated substrates were rinsed extensively with deionized water, and the water contact angles were determined by fluorescence microscopy at different excitation wavelengths (405, 488, and 543 nm).

MTT assay

The biocompatibility of CD and Cu^{2+}-CD was investigated using MDAMB and MDCK cells via an MTT assay. In particular, a 200-µL volume of cell solution containing 2×10^5 cells/mL was cultured in 96-well plates and then incubated at 37 °C for 24 h in a humidified 5% CO_2 environment. The cellular viability was determined by dissolving materials in RPMI medium at different dilutions (0.01–1 mg/mL) and subsequently incubating with cells prepared in the previous step for another 24 h. The medium was then replaced with 180 µL of fresh RPMI medium and 20 µL of a stock MTT solution (5 mg/mL); the samples were incubated for another 4 h. Finally, 200 µL of MTT solubilizing agent was added after removing the medium, followed by a 15-min shaking step. The absorbance was then measured at 570 nm.

Selectivity assessment for the PPi sensing assay

To assess the selectivity of the biosensor for PPi, different anions, including Cl^-, Br^-, I^-, SO_4^{2-}, OH^-, PO_4^{3-}, HS^- and PPi were used. A certain amount of each anion (10 mM) was introduced into the Cu^{2+}-CD solution (1 mg/mL) prepared as described above, and then fluorescence spectra were monitored at the excitation wavelength of 380 nm.

Membrane and nucleus imaging in aqueous and coated surface states

Briefly, MDAMB and MDCK cells were seeded onto a cover slide at a density of 2×10^5 cells/mL and were then incubated for 24 h at 37 °C in a humidified atmosphere with 5% CO_2. They were then treated with Cu^{2+}-CD (1 mg/mL), and a washing step was performed three times to remove free cells. Next, the samples were stained with CellBrite™ Cytoplasmic Membrane Dyes (Green) and Syto 61 Red, followed by the addition of PPi (100 µL) and ALP (1000 U/L). Finally, after 4 h, the stained cells were analyzed using a LSM510 confocal laser-scanning microscope (Carl Zeiss, Germany).

For solid state confocal microscopy, 1 mL of RPMI medium containing 2×10^5 cells was seeded over the coated PET surface in a six-well dish, and incubated for 24 h under the above conditions. The cells were then washed with phosphate-buffered saline (PBS) and stained with membrane marker (green) following the addition of PPi (100 µL) and ALP (1000 U/L). Finally, the cellular uptake was observed using a LSM510 confocal laser scanning microscope at a magnification of 20 ×. The cells were then collected in an EDTA solution and centrifuged. The obtained cells were examined using a LSM510 confocal laser-scanning microscope. To further confirm the effect of ALP on the fluorescence-off behavior, we added an ALP inhibitor and incubated for 30 min, after which the cells were collected and examined by confocal microscopy.

Flow Cytometry Analysis

MDAMB and MDCK cells were cultured in six-well plates at a density of 1×10^6 cells/mL per well under humidified 5% CO_2 environment at 37 °C. After 24 h, the medium was replaced with C/C_{12}-SP, CD, and Cu^{2+}-CD in RPMI and incubation was continued for the designated time. The cells were then collected and resuspended in 1% FBS in PBS solution with a pH of 7.4. The mixture was analyzed using an Attune NxT Acoustic Focusing Cytometer at an excitation wavelength of 405 nm and an emission wavelength of 450 nm.

RESULTS AND DISCUSSION

Developing selectively targeted biosensors that differentiate between normal and cancer cell is an important challenge for the early diagnosis and treatment of tumors. In the present study, we describe a fluorescent OFF-ON-OFF-based system for membrane-/nucleus tumor-specific sensing that exploits changes in the chemical nature of cells. As illustrated in Scheme 1(a), the designed system for membrane/nucleus selective tumor detection based on PPi and ALP activity assays was prepared using carbonized C/C_{12}-SP to allow tumor-triggered detection assays on different mediums. The hydrophobic group of the CD can effectively penetrate into the lipid bilayer of a membrane via hydrophobic interactions. After entering the cancer cell, the zwitterion group of CD changes to strong hydrophilicity in an acidic environment, causing nuclear translocation of the CD (Scheme 1(b)). This proposed assay has a robust ability to selectively analyze tumor cells in response to intracellular PPi and ALP activity with high sensitivity and provides a rapid colorimetric assay for further clinical diagnostics, making it superior to traditional sensors.

As shown in Scheme 1(a), the strong acid H_2SO_4 was used to prepare the C/C_{12}-SP to obtain the CD system. To verify the structural components of the CD platform, the ^{1}H-NMR spectra were evaluated (Fig. 1(a)). The appearance of the peaks at approximately 2.2–3.0 confirmed the integrated sulfobetaine and C_{12} groups on the PEG carbon chains.

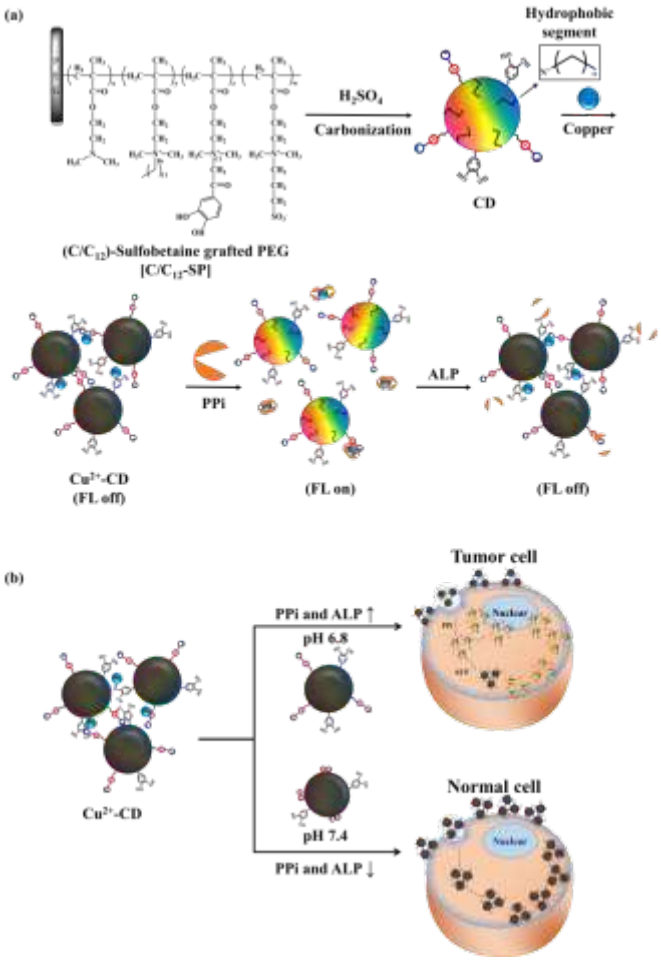

Scheme 1. (a) Schematic illustration of the fluorescent assay for tumor selective detection based on Cu^{2+} functionalized carbon dots (CD) in response to pyrophosphates (PPi) and alkaline phosphatase (ALP), and (b) the endocytosis mechanism of Cu^{2+}-CD to detect cancer cells.

The intense peaks at 7.2–8.0 were assigned to the aromatic moieties of the catechol groups (10 units). In the ^{1}H NMR spectra, the peaks observed after the carbonization process were similar to those observed before carbonization, indicating that the structure of the material was maintained during the dehydration process. Additionally, the integration of the catechol group was recorded via UV-Vis spectroscopy to investigate the optical properties of the prepared CD. As shown in Fig. 1(b), the aqueous solution of C/C_{12}-SP and CD showed similar UV absorption peaks at 280 and 360 nm, which

DOI: 10.1039/C8TB01764K

are attributed to the π-π* transition of the aromatic sp2 domains of carbonized species and the n-π* transition of the C=O bond of the catechol groups, which remained stable even after Cu^{2+} chelation.[25,27] To verify the structure of the zwitterionic sulfobetaine group would change to the fluorescence characteristics of CD depending on pH, the PL spectra was observed (Fig. S1(a)). At physiological pH (7.4), self-quenching of the CD fluorescence via the aggregation-caused quenching (ACQ) phenomenon was observed, because the sulfobetaine group increased the hydrophobicity of the CD, thus, promoting aggregation. Under acidic conditions, the sulfobetaine groups on the nanoparticle surfaces are protonated and ionized, thereby, increasing their hydrophilicity, resulting in relatively high-intensity fluorescence. In a basic environment, the fluorescence of the CD was quenched because of auto-polymerization of the catechol residues, which resulted in effective fluorescence quenching ability. The structure of zwitterionic groups under different pH conditions was also evaluated by DLS (Fig. S1(b)). The average size of the CD was 137.5 nm at pH 7.4, which decreased to ~ 50–60 nm at pH 6.8 and 9.0, indicating the breakdown of the aggregation of zwitterion groups. To further validate the successful interaction between CD and Cu^{2+}, the sample composition was analyzed using XRD spectroscopy Fig. 1(c). XRD verified the presence of Cu^{2+} on the CD platform, since the 2θ value of the peaks is in the range of 40–60 and 70°, confirming the confirming the integration of Cu^{2+}. After the addition of PPi into the Cu^{2+}-CD system, peaks at 35, 38, and 58° appeared, providing evidence for presence of Cu^{2+} as typical O chelated ligands on PPi.

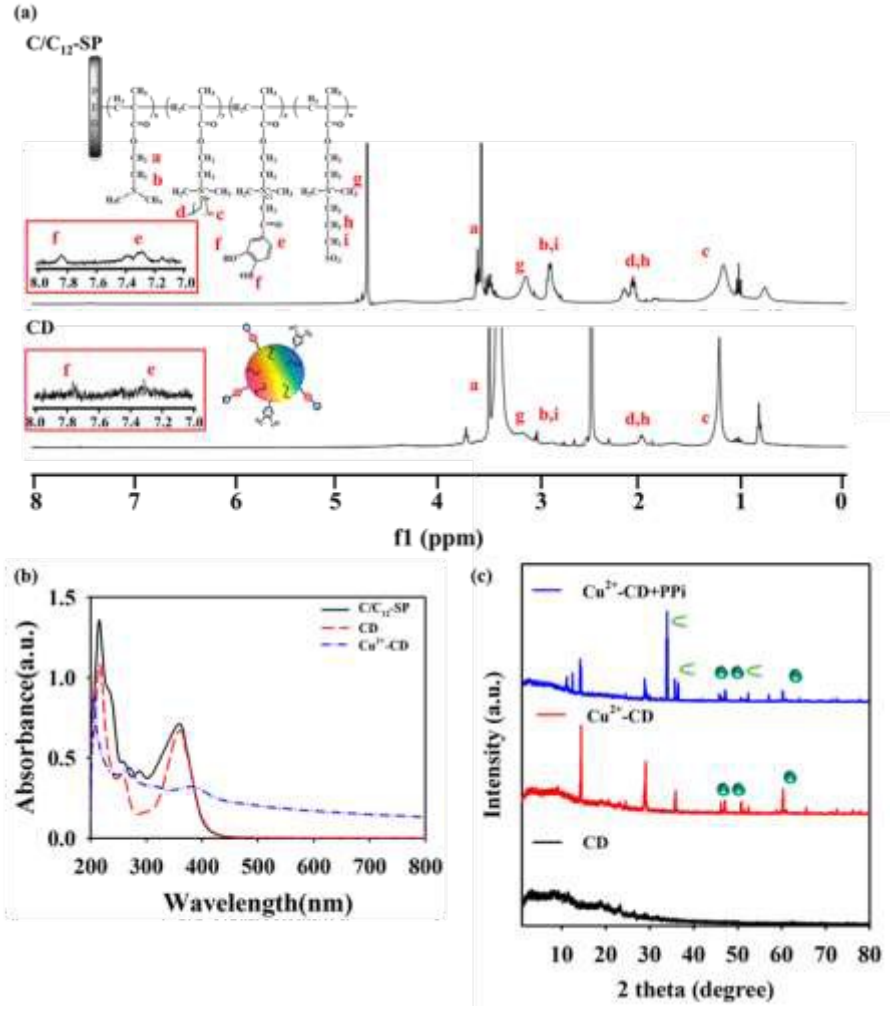

Fig. 1. (a) ^1H NMR spectra (400 MHz, D_2O) of C/C_{12}-SP and carbon dots (CD) (b) Ultraviolet-visual-near infrared absorption spectra of C/C_{12}-SP, CD, and Cu^{2+}-CD at 1 mg/mL concentration. (c) XRD spectra of CD, Cu^{2+}-CD, and Cu^{2+}-CD with the addition of PPi.

Cu^{2+} were reported to act as molecular glue and/or quenchers, which can rapidly complex with CD via self-assembly.[16] To verify the aggregation, DLS analysis was investigated as shown in Fig. 2(a). After complexation with Cu^{2+}, the CD size obvious increased from 137 to 252.7 nm in which SEM images shown in Fig. 2(b) clearly proposed the aggregation of CD by Cu complexation. It was obviously showed the dot shaped became aggregate in the presence of Cu^{2+}. While interact with PPi, the sample returned to previous size as CD. The aggregation was re-occurred when the

nanoparticle interacted with ALP. Moreover, we observed PL spectra of CD in Fig. 2(c), in the presence of Cu^{2+}, the fluorescence of the CD was almost completely quenched. The dependence of the fluorescence quenching effect on the concentration of the Cu^{2+} is shown in Fig. S2(a); we observed a decrease in the quenching of fluorescence as the concentration of Cu^{2+} increased. To verify the stronger affinity of PPi for Cu^{2+}, we also investigate the PL spectra of Cu^{2+}-CD after the addition of PPi dependent on concentration. They show that the addition of PPi (100 μL) anions caused fluorescence recovery to about 80% of the initial CD fluorescence compared with other concentrations (Fig. S2(b)). Thus, the fluorescence recovery showed that PPi can preferentially capture Cu^{2+} inside the aggregated CD because of their stronger affinity for Cu^{2+} compared with that of the carboxylate groups on the CD. The CD would then disaggregate to generate free CD, thereby recovering the fluorescence intensity.[22] Finally, varying concentrations of ALP were introduced into the Cu^{2+}-CD+PPi solution after 20 min of incubation. As shown in Fig. S2(c), re-quenching of the fluorescence of the Cu^{2+}-CD+PPi solution was observed, with a greater quenching at higher ALP concentrations (1000 U/L). This confirmed that ALP hydrolyzed the PPi into phosphate anions and released the Cu^{2+} from the PPi-Cu^{2+} complexes. Moreover, we confirmed that this phenomenon was truly a consequence of ALP catalysis using an ALP inhibitor solution (Na_3VO_4). The fluorescence intensity of Cu^{2+}-CD+PPi was stable after the addition of the inhibitor, suggesting that fluorescence quenching was inhibited by blocking the ALP activity (Fig. 2(c)).[35] Furthermore, the Cu^{2+}-CD was analyzed using DLS under different pH solution (6.8, 7.4 and 9.0) solution as shown in Fig. 2(d). Fig. 2(d) did not give any obvious changes in response to pH, indicating the aggregation of CD by copper disturb zwitter ionic structure.

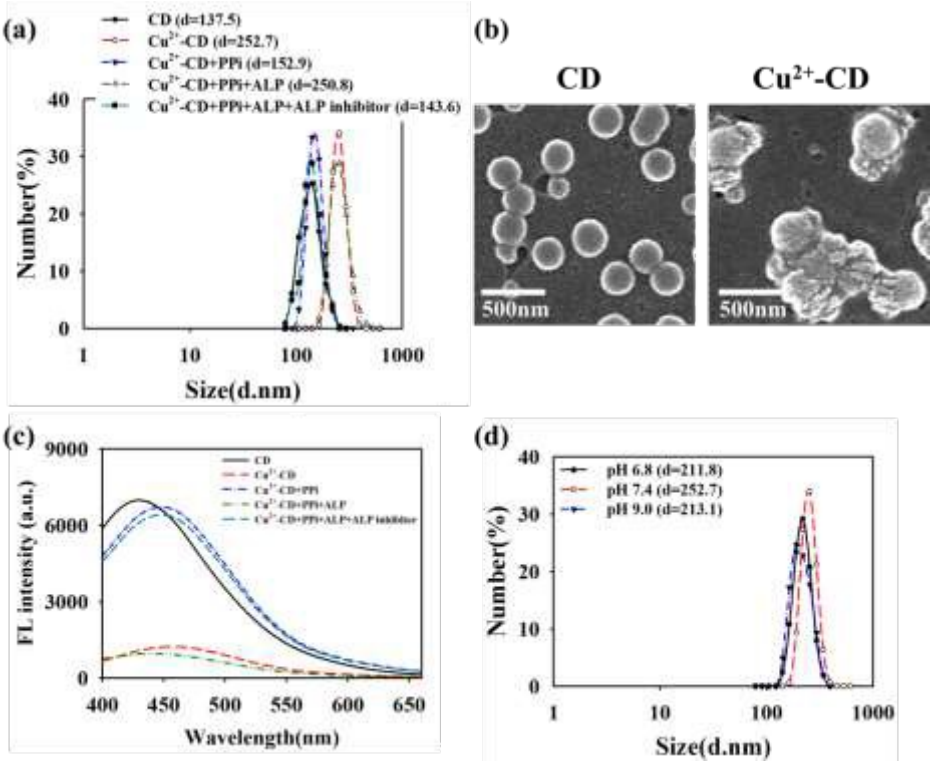

Fig. 2. (a) DLS measurements of CD, Cu^{2+}-CD, and Cu^{2+}-CD with the addition of PPi, ALP and ALP inhibitor in 0.01 mg/mL concentration. (b) SEM images of CD and Cu^{2+}-CD. (c) Fluorescence emission intensity of CD, Cu^{2+}-CD, Cu^{2+}-CD+PPi, Cu^{2+}-CD+PPi+ALP, and Cu^{2+}-CD+PPi+ALP+ALP inhibitor (1 mg/mL) at an excitation wavelength of 380 nm. (d) DLS of Cu^{2+}-CD for determining the changes in the distribution of the hydrodynamic radius in different pH solutions CD.

We verified the activity of the fluorescent OFF-ON-OFF system by flow cytometry (Fig. 3(a)). Fig. 3(a) shows a fluorescence mean value in the switch "OFF" condition of 639 for the CD, which decreased to 227 after Cu^{2+} complexation[22], but totally recovered after the addition the PPi. This occurs because one copper binds to several carboxyl groups on the surfaces of the CD *via* complexation and metal coordination, resulting in intense aggregation of the CD, leading to significant quenching via the ACQ process.[36] The addition of PPi restored the fluorescence intensity of CD because PPi preferentially binds to Cu^{2+}. Once ALP was added, the PPi were effectively hydrolyzed, releasing the Cu^{2+}, which resulted in the intense fluorescence of CD being quenched again because of the re-aggregation of the CD *via* the ACQ process. To evaluate

the selectivity of Cu^{2+}-CD towards PPi, we evaluated the fluorescence emission of Cu^{2+}-CD upon addition of various anions, including Cl^-, Br^-, I^-, SO_4^{2-}, OH^-, PO_4^{3-}, HS^- and PPi (Fig. 3(b)). The addition of Cl^-, Br^-, I^-, SO_4^{2-}, and OH^- did not induce fluorescence recovery; however, some recovery of quenching was observed upon the addition PO_4^{3-} and HS^-, indicating the possibility that Cu could complex with PO_4^{3-} and HS^-. As expected, the presence of PPi caused specific fluorescence enhancement. Although PO_4^{3-} and HS^- showed some fluorescence enhancement, the Cu^{2+}-CD have great selectivity for PPi, as indicated by the sharp increasing in fluorescence in the PPi solution, suggesting that these other anions would not interfere with PPi sensing.

For further biological applications, biocompatibility is an important parameter in a medicinal material. MTT assays were performed to evaluate the toxicity of the CD probes towards MDCK and MDAMB cells. As expected, the cell viability of MDCK and MDAMB cells remained at ~100% after interaction with CD at concentrations up to 0.10 mg/ml (Fig. 3(c–d)). Moreover, the addition of Cu^{2+} to the CD system was not toxic to the cells (cell viability remained at ~98%). Thus, the as-prepared Cu^{2+}-CD was considered to have low toxicity and is biocompatible in living cells.

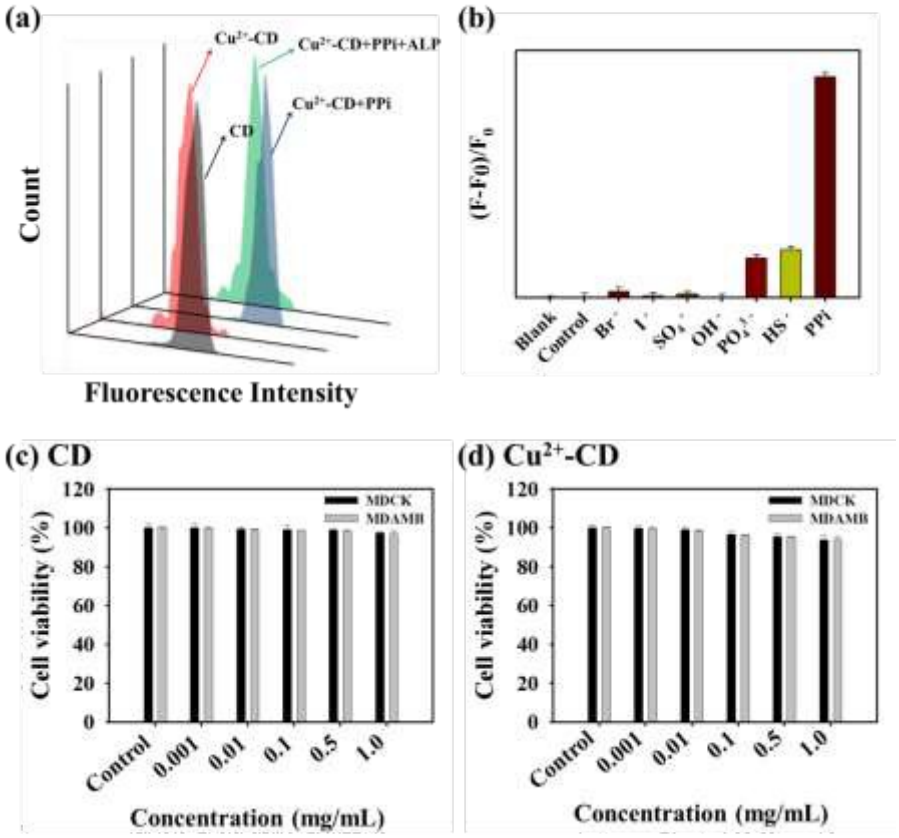

Fig. 3. (a) Flow cytometry analysis of C/C_{12}-SP, CD, Cu^{2+}-CD, Cu^{2+}-CD+PPi, and Cu^{2+}-CD+PPi+ALP nanoparticles (b) Relative fluorescence intensity $(F-F_0)/F_0$ of Cu^{2+}-CD in the presence of different anions. The concentration of each anion was 10 mM (100 µL). (c–d) Concentration-dependent MTT assay for cell viability after treatment with different concentrations of CD and Cu^{2+}-CD nanoparticles.

Our CD system has adhesive properties, and there has been no report of cancer cell detection by monitoring PPi and ALP activity on coated surfaces using fluorescence on/off assays. Therefore, we proposed a new sensing method for cancer cells in a coated state using a simple dip-coating method. The CD was coated on Si wafers and polymeric surfaces, PET, PVC, and PP, and their adhesion was confirmed by determining the water contact angle of the hydrophobic–hydrophilic interactions. As shown in Fig. 4(a), a remarkable decrease in contact angles was observed for the CD-coated surfaces, which indicated that our nanomaterials were more hydrophilic than these versatile surfaces because of the tertiary amine groups of the DMA residues and the sulfobetaine residues of the zwitterionic conformation, all of

View Article Online
DOI: 10.1039/C8TB01764K

which improved the wettability of the coated surfaces. A slight increase in the contact angle on the Si wafer surface revealed that the synthesized CD coating material was less hydrophilic than the bare Si wafer surface. Moreover, the addition of Cu^{2+} and PPi did not have a specific effect on the water contact angle property. The PPi and ALP activity of the coated PET film was assessed by changes in the fluorescence patterns, which were analyzed by fluorescence microscopy. Fig. 4(b) shows that the bare PET did not emit fluorescence. However, after coating with CD, the fluorescent signal was detected as blue, green, and red fluorescence at 405, 488, and 543 nm, respectively. When the Cu^{2+}-CD coated surfacewas examined, we observed the fluorescence OFF state. As observed in the solution state, the addition of PPi resulted in recovery of fluorescence, while the addition of ALP caused the re-quenching phenomenon.

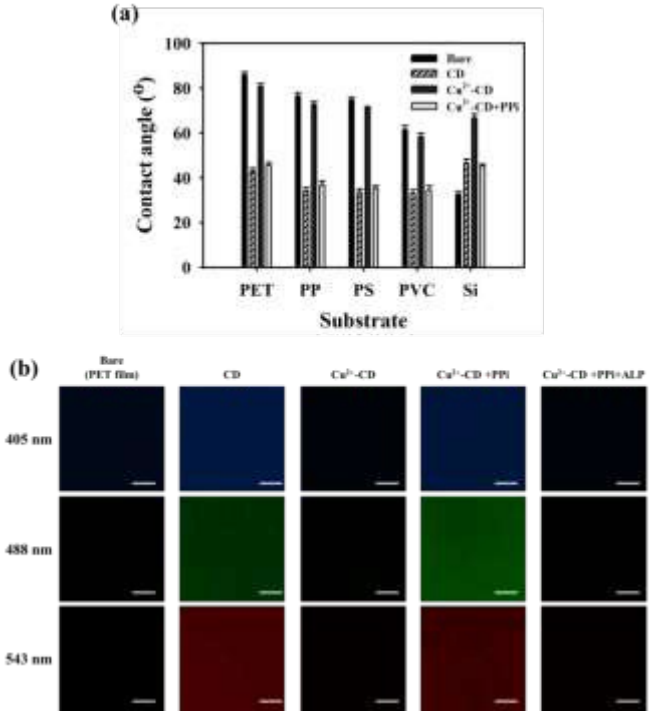

Fig. 4. (a) Water static contact angle (deg) analyses of bare substrates, CD, and Cu^{2+}-CD coated substrates before and after adding PPi solution (100 µL). (b) Fluorescence microscopy images of (a) CD and Cu^{2+}-CD coated PET substrate in the presence of PPi solution (100 µL) and ALP (1000 U/L) at blue, green, and red wavelengths.

Generally, PPi and ALP are intracellularly located, and their levels are different between normal and cancer cells: In cancer cells, the PPi concentration is 100–1300 pmol/10^6 cells and abnormally high levels of ALP (more that 40–150 mU/mL) are present[37,38]. Endogenous monitoring of PPi levels and ALP activity in cancer (MDAMB) and normal (MDCK) cells was performed through time-dependent confocal imaging as a method for tumor detection (Fig. 5 (a, b)), in which the cells were incubated with 1 mg/mL of Cu^{2+}-CD solution for 30 minutes. As a control, fluorescence quenching of Cu^{2+}-CD was observed at 0 min of incubation in both cell lines, while the recovery of fluorescence of the Cu^{2+}-CD biosensor in the MDAMB cancer cells began at 10 minutes and disappeared again after 20 min of incubation. By contrast, the confocal images of MDCK treated with Cu^{2+}-CD showed stable fluorescence OFF during the 30-min incubation. PPi localized in cancer cells will capture the Cu^{2+} in the CD system and form the PPi-Cu complex. This mechanism would break the CD aggregation mediated by Cu^{2+} to generate free CD, resulting in high fluorescence emission. During the first 10 min of incubation, Cu^{2+}-CD interacts with PPi, resulting in fluorescence recovery. After 20 min, the intracellular ALP hydrolyzes the PPi to phosphate ions, which releases the Cu^{2+}, which then re-combine with CD, causing them to aggregate and resulting in another cycle of fluorescence quenching. To verify that the ALP activity in the cells hydrolyzed the PPi, we also analyzed the confocal images of Cu^{2+}-CD-treated cancer cells incubated with the ALP inhibitor. As shown in Fig. S3, the re-quenching behavior was observed, confirming that the PPi could not be hydrolyzed because of inhibition of ALP activity. The penetration behavior of hydrophobic CD is essential for the cellular uptake mechanism, which ensures that our nanoparticles enter the cells, resulting in high particle clearance rates, which can be a reason for disappointing imaging and therapeutic efficacy. Therefore, we used a membrane marker as a control (membrane co-staining-based

View Article Online
DOI: 10.1039/C8TB01764K

fluorescence) to investigate whether the Cu^{2+}-CD were embedded within the lipid bilayer in both cell lines. During 30 min of incubation, the Cu^{2+}-CD were localized on the surface of the cell and fused with the cell membranes, which was confirmed in confocal images of cells treated with the membrane marker. The fluorescence of the CD was distributed on the periphery of the MDAMB and MDCK cells, as shown in the merged confocal images, suggesting the occurrence of a hydrophobic interaction between long chain carbons of the CD with the cell membrane.[39]

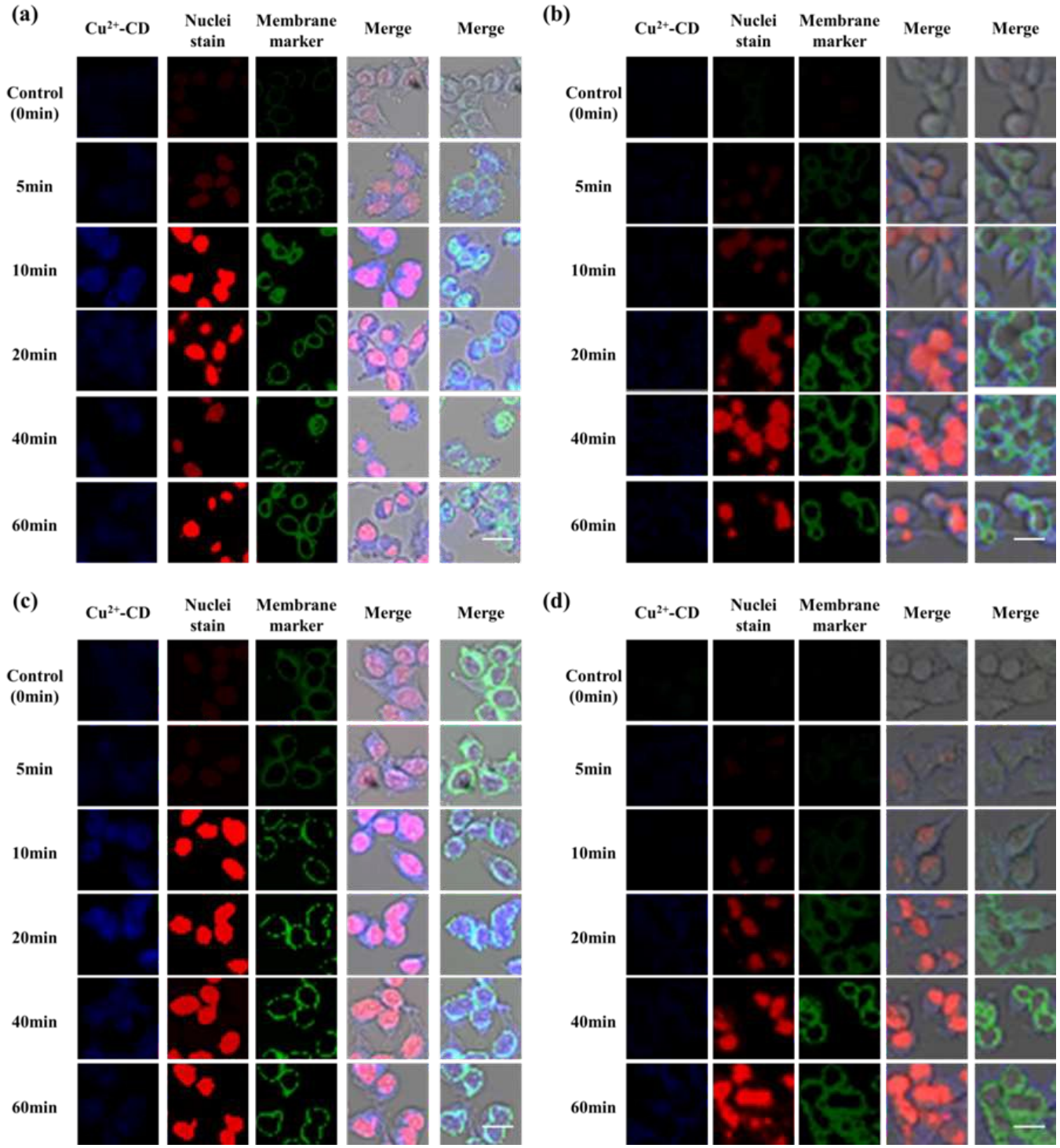

Fig. 5. Confocal laser scanning microscope (CLSM) images of (a,c) MDAMB and (b,d) MDCK cells incubated with Cu^{2+}-CD, nuclei stain and membrane marker for 0, 5, 10, 20, 30, 40, and 60 min. The scale bars represent a distance of 50 μm. The Figure (a), (b) was treated with Cu^{2+}-CD solution (1 mg/mL), and (c), (d) was treated on coated PET with Cu^{2+}-CD.

View Article Online
DOI: 10.1039/C8TB01364K

Furthermore, selective nuclear intracellular uptake of the nano-particles was evaluated by confocal microscopy. The confocal images clearly showed time-dependent localization with the CD moving into the nucleus only in the MDAMB cancer cells compared to CD in MDCK cells treated with a nuclear stain. The phenomenon was not observed in MDCK cells because the physiological pH in the normal cells would have no effect on the zwitterion components of the CD. It should be noted that the significant CD internalization in the nuclei of cancer cells occurred because of the low pH in the cancer cells.

We hypothesized that our system involves a two-part endocytosis mechanism. The hydrophobic CD can effectively penetrate into the lipid bilayer of the membrane via hydrophobic interactions; after entering the cancer cell, the zwitterionic component of the CD becomes strong hydrophilic in response to the acidic intracellular pH, resulting in nuclear translocation of the CD.

We further tested the ability of PET coated Cu^{2+}-CD to detect ALP activity by culturing cancer cells on the PET surface (Fig.. 5(c, d)). Fig. 5(c) shows the changes in fluorescence over time of MDAMB cells on coated film. The PPi activity could be detected at 10 min due to recovery of fluorescence. Some minutes later, the ALP activity was also confirmed by the re-quenching of fluorescence. This change in fluorescence behavior was not observed in the normal cells. Subsequently, addition the ALP inhibitor reduces the ALP activity abrogated the re-quenching process of the Cu^{2+}-CD inside the cells coated on PET (Fig. S3). Thus, we demonstrated that the present system could be used to monitor the PPi levels and ALP activity within cells through fluorescence imaging with diverse substrates.

To confirm that the fluorescence response to Cu^{2+}-CD in MDAMB and MDCK cells is different, we examined confocal images of MDCK cells cultured after addition of the PPi and ALP solution in an acidic pH (6.8) environment (Fig. S4 and S5). The recovery of fluorescence was observed after the addition of PPi, and the fluorescence intensity decreased again after the addition of the ALP solution. This confirmed that the normal cells did not contain high levels of PPi and ALP, because the Cu^{2+}-CD response was observed only on the addition of exogenous PPi and ALP. Moreover, to determine why the CD system cannot translocate into the nuclei of MDCK cells, we further incubated the MDCK with Cu^{2+}-CD under acidic pH (6.8) for 30 min. The Cu^{2+}-CD translocated to the nucleus under acidic conditions as compared with cells treated with the nuclear stain only. Therefore, we hypothesized that the CD enter the nucleus through the nuclear pore complex because the surface charges of the zwitterion become very hydrophilic in acidic pH, and because of the activity of the histone nuclear import-associated complex.[39] Finally, the strategy developed shows remarkable advantages as a smart material on coated surfaces to monitor PPi/ALP activity in tumor triggered fluorescence assays and could have a great potential for the early diagnosis of various severe diseases.

Conclusions

We prepared a label-free real time fluorometric assay for a membrane and nucleus-targeted tumor specific fluorescence sensing system using hydrophobic and zwitterionic group functionalized CD with Cu^{2+}. The system could be used to monitor the levels of PPi and ALP activity for cancer cell detection. The abundance of carboxyl groups on the CD enables the interaction with Cu^{2+}, which results in aggregation, leading to fluorescence quenching. The tumor-selective fluorescence sensing system showed different transport from the cytosol to the nucleus in normal and tumor cells, which depended on the pH response of the zwitterionic CD, including hydrophobic CD-mediated cell membrane targeting. In human MDAMB cancer cells, the interaction between the CD and Cu^{2+} was disrupted by competitive binding, with stronger affinity of intracellular PPi for Cu^{2+} inducing enhanced fluorescence. A few minutes later, the hydrolysis of the PPi-Cu^{2+} complexes by intracellular ALP in the cytoplasm released the Cu^{2+}, which resulted in re-aggregation of the CD, leading to fluorescence quenching again. The adhesive catechol in the CD provided a novel aspect to our design, allowing detection of cancer cells on coated surfaces. Thus, the system could be used for cancer diagnosis in both aqueous states and on coated surfaces through changes in fluorescence behavior. This biosensor has an apparent potential as a simple and sensitive cancer diagnostic tool that can differentiate between normal and cancer cells on coated surfaces and in the aqueous state.

Conflicts of interest

There are no conflicts to declare.

Acknowledgements

This research was supported by Grant No. 10062079 from the Ministry of Trade, Industry & Energy (MOTIE) and the Basic Science Research Program through the National Research Foundation of Korea (NRF) funded by the Ministry of Education (NRF-2017R1A2B2002365 and 2018R1A6A1A03023788).

References

1 E. Y. K. Ng, *Int. J. Therm. Sci.,* 2009, **48**, 849-859.
2 A. Kowalik, M. Kowalewska, S. Gozdz, *Transl. Res.,* 2017, **185**, 58-84.
3 Y. Wang, Y. Xie, J. Li, Z. H. Peng, Y. Sheinin, J. Zhou, D. Oupický, *ACS Nano,* 2017, **11**, 2227-2238.
4 X. Guan, *Acta Pharm. Sin. B,* 2015, **5**, 402-418.
5 A. Borrelli, A. L. Tornesello, M. L. Tornesello, F. M. Buonaguro, *Molecules,* 2018, **23**, 295.
6 Y. Chen, Z. H. Zhang, X. Han, J. Yin, Z. Q. Wu, *Macromolecules,* 2016, **49**, 7718−7727.
7 G. M. Cooper, R. E. Hausman, *The cell: A Molecular Approach*, Sinauer Associates Inc., Sunderland, U.S.A., 2016.
8 A. Asati, S. Santra, C. Kaittanis, J. M. Perez, *ACS Nano,* 2010, **4**, 5321–5331.
9 J. McMillan, E. Batrakova, H. E. Gendelman, *Prog. Mol. Biol. Transl. Sci.*, 2011, **104**, 563–601.

View Article Online
DOI: 10.1039/C8TB01364K

10 X. Li, Y. Tang, L. Xu, X. Kong, L. Zhang, Y. Chang, H. Zhao, H. Zhang, X. Liu, *RSC Adv.,* 2017, **7**, 33502.
11 B. Yameen, W. I. Choi, C. Vilos, A. Swami, J. Shi, O. C. Farokhzad, *J. Control. Release,* 2014, **190**, 485–499.
12 E. B. Kang, J. E. Lee, J. H. Jeong, G. Lee, I. In, S. Y. Park, *J. Ind. Eng. Chem.,* 2016, **33**, 336-344.
13 Y. Ye, Y. Zheng, C. Ji, J. Shen, M. Yin, *ACS Appl. Mater. Interfaces,* 2017, **9**, 4534−4539.
14 T. Mosaiab, C. Shin, P. H. Choi, G. J. Shin, S. Lee, K. H. Choi, E. S. Yoo, J. Lee, I. In, S. Y. Park, *New J. Chem.*, 2013, **37**, 3845-3848.
15 C. Chen, D. Zhao, J. Sun, X. Yang, *ACS Appl. Mater. Interfaces,* 2016, **8**, 29529−29535.
16 Z. Wang, X. Yu, F. Li, F. Kong, W. Lv, W. Wang, *J. Mater. Chem. B*, 2018, **6**, 1771-1781.
17 K. A. Lomashvili, P. Garg, S. Narisawa, J. L. Millan, W. C. O'Neill, *Kidney Int.*, 2008, **73**, 1024–1030.
18 M. P. Whyte, M. Landt, L. M. Ryan, R. A. Mulivor, P.S. Henthom, K. N. Fedde, J. D. Mahuren, S. P. Cobum, *J. Clin. Invest.,* 1995, **95**, 1440–1445.
19 Y. V. Bobryshev, A. N. Orekhov, I. Sobenin, D. A. Chistiakov, *Curr. Pharm. Des.*, 2014, **20**, 5821-8.
20 U. Sharma, D. Pal, R. Prasad, *Ind. J. Clin. Biochem.*, 2014, **29**, 269–278.
21 A. Váradi, K. Fülöp, T. Arányi, F. Szeri, *Ann. Transl. Med.*, 2017, **5**, 1-489.
22 Y. Hu, X. Geng, L. Zhang, Z. Huang, J. Ge, Z. Li, *Sci Rep.*, 2017, **7**, 1-9.
23 A. Balaji, J. Zhang, *Cancer Nanotechnol.,* 2017, **8**, 10.
24 Y. He, B. Jiao, *Microchim. Acta,* 2017, **184**, 4167–4173.
25 S. M. Sharker, S. M. Kim, J. E. Lee, J. H. Jeong, I. In, K. D. Lee, H. Lee, S. Y. Park, *Nanoscale,* 2015, **7**, 5468-5475.
26 P. G. Luo, S. Sahu, S. Yang, S. K. Sonkar, J. Wang, H. Wang, G. E. LeCroy, L. Cao, Y. Sun, *J. Mater. Chem. B,* 2013, **1**, 2116-2127.
27 E. B. Kang, I. In, K. D. Lee, S. Y. Park. *J. Ind. Eng. Chem*., 2017, **55**, 224–233.
28 C. A. Choi, J. E. Lee, Z. A. I. Mazrad, I. In, J. H. Jeong, S. Y. Park, *J. Ind. Eng. Chem.*, 2018, **63**, 208-219
29 Y. Zou, F. Yan, L. Dai, Y. Luo, Y. Fu, N. Yang, *Carbon,* 2014, **77**, 1148-1156.
30 M. Deng, S. Wang, C. Liang, H. Shang, S. A Jiang, *RSC Adv.*, 2016, **6**, 26936.
31 E. Castanie, M. Boffety, R. Carminati, *Opt. Lett.,* 2010, **35**, 291-293.
32 E. Dulkeith, A. C. Morteani, T. Niedereichholz, T. A. Klar, J. Feldmann, *Rev. Lett.,* 2002, **89**, 23002-4.
33 V. N. Pustovit, T. V. Shahbazyan, *J. Chem. Phys.,* 2012, **136**, 204701-6.
34 L. Zhao, L. Zhao, Y. Miao, C. Liu, C. Zhang, *J. Anal. Methods Chem.*, 2016, **2016**, 1-10.
35 E. B. Kang, C. A. Choi, Z. A. I. Mazrad, S. H. Kim, I. In, S. Y. Park, *Anal. Chem.* 2017, **89**, 13508–13517.
36 X. Ma, R. Sun, J. Cheng, J. Liu, F. Gou, H. Xiang, X. Zhou, *J. Chem. Educ.*, 2015, **93**, 345–350.
37 G. J. Peters, E. Laurensse, A. Leyva, H. M. Pinedo, *Int. J. Biochem.*, 1985, **17**, 95-99.
38 J. Ozer, M. Ratner, M. Shaw, W. Bailey, S. Schomaker, *Toxicology*, 2008, **245**, 194-205.
39 Y. K. Jung, E. Shin, B. S. Kim, *Sci. Rep.*, 2015, **5**, 18807.

View Article Online
DOI: 10.1039/C8TB01364K

Graphical Abstract

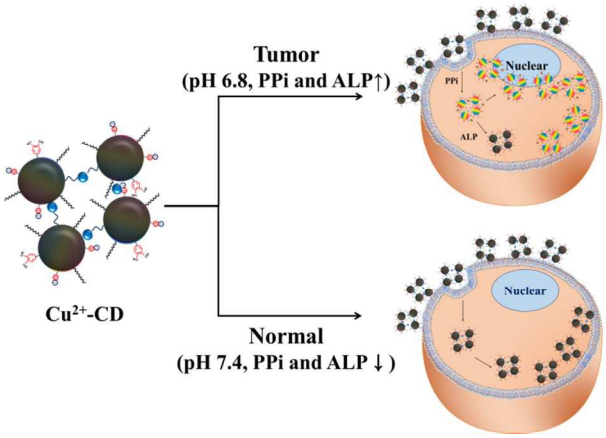

Fluorescence-switching of Cu^{2+}-CD for specific membrane and nucleus targeting based on PPi and ALP activity in tumor cell.